Effect of carbon black nanoparticle intrinsic properties on the self-monitoring performance of glass fibre reinforced composite rods

Francesca Nanni, Giovanni Ruscito, Debora Puglia, Andrea Terenzi, J.M. Kenny, Gualtiero Gusmano

Effect of carbon black nanoparticle intrinsic properties on the self-monitoring performance of glass fibre reinforced composite rods

Francesca Nanni, Giovanni Ruscito, Debora Puglia, Andrea Terenzi, J.M. Kenny, Gualtiero Gusmano

PII: S0266-3538(10)00323-4
DOI: 10.1016/j.compscitech.2010.08.015
Reference: CSTE 4796

To appear in: *Composites Science and Technology*

Received Date: 31 March 2010
Revised Date: 14 August 2010
Accepted Date: 21 August 2010

Please cite this article as: Nanni, F., Ruscito, G., Puglia, D., Terenzi, A., Kenny, J.M., Gusmano, G., Effect of carbon black nanoparticle intrinsic properties on the self-monitoring performance of glass fibre reinforced composite rods, *Composites Science and Technology* (2010), doi: 10.1016/j.compscitech.2010.08.015

Effect of carbon black nanoparticle intrinsic properties on the self-monitoring performance of glass fibre reinforced composite rods

Francesca Nanni [1,*], Giovanni Ruscito[1], Debora Puglia[2], Andrea Terenzi[2], J.M. Kenny[2] and Gualtiero Gusmano[1]

[1]INSTM research unit of - Dept. of Sciences and Chemical Technologies, Univ. of Rome "Tor Vergata"- Via della Ricerca Scientifica snc – 00133 Roma (Italy)

[2]Dept. of Civil and Environmental Engineering ,Univ. of Perugia – INSTM/NIPLAB – Loc. Pentima Bassa 21 – 05100 Terni (Italy)

Abstract – Self-monitoring composite rods, made of an internal conductive core surrounded by an external structural skin, were manufactured and tested. Both parts were made of glass fibre-epoxy Electrical conductivity was achieved in the inner core by incorporating as an alternative high surface area or low surface area carbon black in the resin. Self-monitoring performance was assessed by simultaneous mechanical and electrical resistance measurements. The aim was to correlate the electrical resistance variation to stress. Only one type of material showed appropriate self-monitoring properties, since increase of electrical resistance was recorded at increasing loading (both monothonic and cyclic tensile loading), while electrical resistance recovery at high loads was found in the other case. Calorimetric analysis, rheological measurements and SEM observations were carried out to explain this result. Filler dispersion seems to

[*] Corresponding author: fax. .+39.06.7259.4328. e-mail: fnanni@ing.uniroma2.it (Francesca Nanni)

be the key feature affecting the self-monitoring properties. Only high surface area nanoparticles can ensure self-monitoring reliability.

Keywords – Self-monitoring (B), polymer-matrix composites (A), pultrusion (E)

1. Introduction

In past years, self-monitoring polymer composite materials were proposed as innovative monitoring systems, that can provide contemporarily structural and sensing properties [1, 2, 3]. Such materials gained particular interest in the field of civil engineering applications, where the use of polymer composite reinforcing rods has become more and more attractive, in order to overcome corrosion problems, typical of steel reinforcements. Usual polymers employed in these applications are epoxy, vinylester-epoxy, polyester, etc. [4]. Polymer composite rods generally present linear elastic failures, i.e. a lack of ductility, which can lead to sudden fractures [5]. Therefore these reinforcements are usually applied together with health-monitoring systems, to prevent catastrophic failures. Both traditional (such as strain gauges, piezoelectrics [6]) and innovative monitoring systems (fibre optics, etc. [7,8]), usually make use of sensors that, placed either inside or outside the concrete structure, are invasive, complicated, expensive and, in the case of external sensor, do not allow continuous monitoring throughout structure service life. To overcome such drawbacks, an alternative monitoring method has been proposed more recently, which makes use of self-monitoring materials, providing both the structural and sensing functions [9,10,11]. Such materials are usually realized with polymer composites, since they offer intrinsic versatility (i.e. possibility to include different phases within the matrix), ease of

fabrication and low costs, which are attractive features for mass production, as in the case of civil engineering. The working principle of self-monitoring materials is based on the correlation between the change of electrical resistance of a conductive phase and the stress/strain occurring to the material [12,13]. In the case of polymeric composites, usually the conductive phase is carbon either in the form of long fibres (CFRP) [14,15,16] or particles (CPRP) [17,18,19] or, more recently nanotubes [20,21]. In the first case, when dealing with unidirectional CFRP rods, carbon fibres can operate both as reinforcement and sensitive part and, therefore, are particularly applied in civil engineering applications, where they are usually used in combination with glass fibres to form hybrid composites (CF-GFRP), that can allow to reach some pseudo-ductility [22,23]. From the monitoring point of view, this solution present low sensitivity at low strains (unless prestressing is provided [12]) and generally low maximum electrical resistance variation (about 10%) until fracture. Therefore the authors in [24] suggested to employ such system as non-continuous health monitoring, and to tailor the composite composition (i.e. glass/carbon fibre ratio) to use this material as a "guard sensor", generating an alarm warning at specific stress. Good self-monitoring results were, instead, obtained in CFRP laminates to monitor cracking and delamination at interlaminar interface [25]. The use of carbon particle as conductive phase, instead, has been more recently proposed and showed good self-monitoring potentialities. Okuhara et al in [26] reported that, differently from CFRP, the introduction of micrometer carbon flakes in the resin allows to achieve more sensitivity, in particular at low strain, and to perform continuous monitoring. This system presents an interesting "memory" function, in the sense that a residual electrical resistance can be found after cyclic loading, that can be somehow correlated to the maximum stress applied to the material. Moreover,

Okuhara et al. in [27] and Inada et al. al [9] observed that carbon particle type and geometrical shape play a significant role in the self-monitoring behaviour. They showed that the use of graphite carbon flakes is particularly suitable for high sensitivity samples, while the use of spherical carbon black particles increase the material capability to memorize maximum applied load. The self-monitoring efficiency of carbon nanoparticles within polymer matrix encouraged and stimulated the research in the more innovative and promising field of carbon nanotube (CNT) loaded polymers [28,29, 30], whose penetration in industrial manufacturing is not shortly expected due to difficulty in CNT manipulation and processing. CNT loaded polymers in the form of film have shown [29,30] to be very promising as strain sensing, but have to be used as external sensors, while good self-monitoring has been achieved in [28] in monitoring delamination of cross-ply laminates with CNT dispersed in the resin. More recently a very interesting work [31] compared the self-monitoring performance of CB-epoxy and MWCNT-epoxy composites and evidenced that self-monitoring in CNT samples shows a distinct dependency of the electrical resistivity on mechanical load, that was attributed to the peculiar nanofiller fibre-like structure.

The different self-monitoring behaviour of CFRP and CPRP systems is related to their different conditions of electrical conductivity, which, in turn, are linked to the material microstructure. In the case of aligned long carbon fibres, the system can be assimilated to a bunch of conductive wires. The electrical current flows either in fibres direction and in transverse direction by means of bridge contacts between neighbouring fibres. This occurrence explains the low sensitivity of such system since, even when some carbon fibres are broken and the longitudinal current flow is obstructed, electrical conductivity is still insured by means of bridge contacts among broken fibres, that allow current flow

in transverse direction [1]. In the case of carbon particles, instead, the electrical model is that of a number of conductors randomly dispersed in an insulating matrix. The theory for such systems reports that conductivity is achieved when a percolation pattern is formed [32,33], i.e. a sufficient numbers of contacts between conductive particles is present to insure current flow. In this conditions, the system quickly changes from being insulator to being conductive. When such system undergoes increasing strain, separation between conductive particles occurs, resulting in higher electrical resistance. Sensitivity is enhanced since the conductive particles gradually separate under strain, with a consequent continuous enhancement of resistivity. Moreover, beyond matrix yielding and after loading, a permanent separation between particles occurs, which generates the "memory effect". In this latter system, the conductivity and, hence the self-monitoring performance, depends on a variety of factors usually related to the peculiar matrix/filler intrinsic properties, such as filler content, intrinsic conductivity, surface area, geometrical shape, etc. [34,35]. Some of these features affect conductivity since they interact with particle dispersion and formation of aggregates, particularly important when dealing with nanofillers. In fact, when carbon nanoparticles (CnP) are mixed to an insulating polymer matrix different mesostructures can appear, depending on the filler intrinsic properties. In particular, it is well known [36] that carbon nanoparticles with high surface area and Oil Absorption Number (OAN) present the so-called "high structure", i.e. highly branched aggregates, which leads to the formation of the conductive network at lower carbon content (low percolation threshold).

In this research two types of hybrid self-monitoring composite rods, made of an internal conductive core surrounded by an external structural part, were manufactured and fully characterized. Both the internal core and the external part were made of glass fibre-

epoxy, nevertheless, electrical conductivity was achieved in the inner core by incorporating carbon nanoparticles within the resin. In particular, the manufactured self-monitoring composite materials contain, as an alternative, two types of carbon black nanoparticles with different surface areas, OAN and particle size. The aim was to correlate the composite self-monitoring performance to the conductive filler properties, by characterizing the filler interaction with the epoxy matrix. Tensile tests were carried out, on both kind of samples, together with electrical resistance measurements, to assess the self-monitoring performance, while their microstructure was observed by field emission scanning electron microscope (FE-SEM). DSC and rheological measurements were performed in order to correlate the measured self-monitoring performance to the material microstructure of both systems. Prior to self-monitoring testing, percolation behaviour of both systems was assessed to find conductivity threshold.

2. Materials and methods

The manufactured composite materials consisted of an internal electrically conductive core surrounded by an insulating sheath (Figure 1).

Figure 1 , **Table 1**

Both parts are made of unidirectional glass fibres (Cofitech, Caselle, Italy, 475W, 2400 tex) in epoxy resin (pure epoxy resin with isofordiammine cycloalifatic hardener, SP system, Gurit, Newport, UK). The manufacturing process is hand-pultrusion. A two-step process was employed: first a glass fibre bundle was pulled through the epoxy resin previously loaded with carbon particles to gain the necessary electrical conductivity, further three additional glass fibres were pultruted around the central conductive core to obtain the insulating sheath and to insure good mechanical properties. Cure reaction was

carried out at 60°C for 3h. Table 1 reports the main characteristics of the realized samples. In final specimens the internal conductive core was made longer than the external sheath to provide electrical contacts, that were applied at specimen ends using a highly conductive silver paint (Electrolube), to allow electric resistance variation measurements (digital multimiter Keithley DMM 2700). The electrical resistance of both wires and contacts between wires and specimens surface is included in the two-points measurement scheme adopted. Nevertheless, preliminary electrical resistance measurements carried out with both two-points and four-points methods showed a difference in specimen resistance evaluation of around 1 Ω that, being far lower than the specimens electrical resistance (table 4), can be considered negligible [30, 37]. Specimens ends were provided of external metallic cylindrical tabs for tensile testing (Figure 1a). In Figure 1d a particular showing sample gripping in tensile test jig, with the electrical contact above the metallic cylinder not affected by any gripping pressure. The The CnP/resin mixture was prepared by adding the particles to the resin and mechanically stirring at 600 rpm for 1h. Successively the hardener was added to the mixture (38 phr) that was kept under mechanically stirring for further 5 min and sent to the pultrusion process. Two types of carbon nanoparticles (Printex XE 2b Evonik-Degussa, Essen, Germany and Super P, Timcal Ltd, Bodio, Switzerland) were used as an alternative to prepare the electrically conductive element: both are spherical carbon black powders with particle average diameters of respectively 30 and 40 nm, but different surface areas. Table 2 reports the main characteristics of the chosen CnP.

Table 2

Percolation was assessed by measuring electrical resistivity of samples with different carbon contents (Keithley DMM 2700) (Table 3). To this aim 10x10x3mm^3 CnP-epoxy

samples [38] were cast in moulds, cured following the above reported procedure, and provided by electrical contacts made of silver paint on opposite sides. Different carbon loadings were chosen in the two types of samples due to the diverse CnP density and efficiency in reaching percolation. The goal was to obtain for the self-monitoring testing samples with similar initial electrical resistance (samples HSA_3 and LSA_4 in Table 3).

Table 3

Table 3

Microstructure of both conductive elements was observed by field emission scanning electron microscope (FE-SEM, Leo Supra 35) to find out the percolation pattern and evaluate filler dispersions. Samples for SEM analysis were microtomed and polished. Monotonic tensile and cyclic tests were carried out at 2 mm/min (Instron 5569J) on hybrid CnP-GFRP composite samples with filler content close to percolation (HSA_3 and LSA_4 samples). In the case of cyclic testing the load was progressively increased following the law: $F_i = F_{(i-1)} + 250$ (N), with F maximum applied load (N) and i, number of cycle. Together with the mechanical tests, electrical resistance variation was acquired (DMM 2700 Keithley Instruments) to assess the self-monitoring performance. Calorimetric measurements were performed to evaluate the interaction between the filler and the pre-polymer, in order to verify whether it could affect the curing behaviour of the epoxy system, with particular attention to the final degree of cure of the material and on the glass transition of fully cured samples. Tests have been carried out using a differential scanning calorimeter (Mettler Toledo 822e, temperature scanning in the range -50°C/250°C, heating rate 10°C/min). Isothermal cure of the three systems (neat epoxy, HSA_3 and LSA_3) was also considered, in order to estimate the final degree of cure of samples, cured for different times at 30, 60 and 90°C.

Rheological tests were carried out with a rotational rheometer ARES with parallel plate geometry (ϕ = 25 mm, frequency sweep test between 0,01 and 100 rad/s at temperature of 30°C and strain of 0,03%), to evaluate and compare the viscosity of the two CNP/epoxy filled systems. In order to minimize the wall effects, the gap within the plates was maintained higher than 100 times the mean particle diameter.

3. Results and discussion

3.1 Percolation

Percolation curves of both systems are reported in Figure 2, while Table 4 reports more in detail samples electrical characteristics.

Figure 2 , **Table 4**

It was found that in the two systems, percolation occurs at different CnP content, respectively at 2.2 %vol (HSA sample) and at 3.8 %vol (LSA sample). Such results are in good agreement (Table 5) with those obtained by applying Janzen equation [39] (eq.1):

$$\Phi_C(Vol\%) = \frac{1}{1 + 4 * \rho * OAN} \qquad (1)$$

which correlates the conductive filler content at percolation with carbon particles OAN and density (ρ).

Table 5

The slight differences found between experimental and theoretical values are in the usual range, as reported in [40], when working with highly structured carbon fillers. Percolation is affected by particles surface area: small surface areas, in fact, correspond to the formation of isolated and compact carbon particle mesostructures, the so-called "low structure" carbon black [32], that difficultly interact to form a conductive network.

Particles with higher surface area, instead, form highly branched agglomerates that more easily interconnect each other [39,40], reaching percolation at lower filler content. Surface area is in turn correlated to the particles diameter: the higher the former, the smaller the latter. The experimental results are consistent with all these considerations. In fact, we found percolation to occur at lower filler content in the case of HSA nanoparticles due to their high surface area, low diameter and high OAN. Moreover, even above percolation, HSA specimens present higher conductivity at lower filler content.

3.2 Self-monitoring assessment

Figure 3, Figure 5a and Table 6 report the self-monitoring performance of a HSA_3 sample. The reported results show a very interesting self-monitoring behaviour, since a strict correlation between mechanical and electrical measurements was found, which make such material suitable for continuous monitoring. Nevertheless, it has to be remarked that this system offers limited sensitivity at low strain (Figure 3), that is however typical of carbon black filled systems [18]. Sensitivity was evaluated at low strain (Figure 5c) by means of the gauge factor (GF), i.e. the ratio between electrical resistance variation and strain ($(\Delta R/R_0)/\varepsilon$). In the case of HSA_3 it is around 6, which is higher than that of usual metal alloys used for foil strain gauges (that lies between 0.7 and 5) [30]. In this system, the self-monitoring performance can be referred to the presence of a network of carbon particles that, prior to loading, allows goods dc electrical conductivity. Successively, the progressive increase of stress and, hence of strain, and/or the inset of damage causes particles separation, resulting in an increase of electrical resistance. Under increasing loading, in fact, always less conductive pathways are available for current flow, with a consequent decrease of conductivity.

Figure 3

In previous work [12] it was evidenced that the abovementioned mechanism of self-monitoring behaviour, implying particle separation at increasing loads, plays an important role in determining system sensitivity (i.e. electrical resistance variation with stress or strain) too. In particular sensitivity at high loads showed to decrease at increasing carbon content, where the high amount of conductive particles always insure enough electrical current flow. Therefore, in this research, specimens with carbon content close to that of percolation were chosen. The good self-monitoring performance is kept even under progressive cyclic loading, where, moreover, the presence of a clear residual electrical resistance after few cycles testifies the ability of such system to memorize maximum applied load, in agreement with what reported in the cited work [9, 17].

Very poor self-monitoring results were found, instead, in LSA_4 samples (Figure 4, Figure 5b and Table 6). In monotonic tensile tests, in fact, the electrical resistance measurements show a self-monitoring behaviour up to about 5000N, above which an evident decrease of electrical resistance was recorded, even under increasing loading. Even system sensitivity at low strain (GF reported in Figure 5 c) is unsatisfying, being around 3, almost the half of that found in the case of HSA_4 sample and in the same range of that of metal alloys. Besides, some loading drops were recorded in the monotonic tensile test (Figure 4), that most probably have to be referred to some debonding occurring between the CnP sensitive part and the external glass skin.

Figure 4

The phenomenon of electrical resistance recovery at high loads was recorded even under cyclic loading, where such occurrence is even more evident: the electrical resistance variation progressively decreases its amplitude, starting from 4500N, up to a

dramatic change at the final cycles, where it is not anymore able to follow the cyclic loading. The recorded electrical resistance recovery can be explained only as an enhancement of electrical conductivity at high loads, which, considering the peculiar mechanism of electrical conductivity in such samples, means that particles, formerly separated, come near and a uniform distribution of carbon nanoparticles is again achieved. To explain the surprising behaviour found in the case of LSA samples two possible, even concomitant, mechanisms were hypothesized. The first one is related to the degree of filler dispersion within the matrix.

Figure 5 , Table 6

An inadequate dispersion implies the presence of carbon nanoparticles agglomerates that can collapse under high loads, releasing carbon nanoparticles (i.e. a larger number of conductive elements dispersed in the matrix), thus increasing system conductivity. Nevertheless, since this behaviour was not observed in the case of HSA_samples, it should be presumed that, in this system, a more efficient filler dispersion was achieved, resulting in a more uniform microstructure. If this hypothesis is correct, this is probably due to the nanoparticles intrinsic properties. A second possible explanation could be found in a different interaction between HSA and LSA nanoparticles and the epoxy resin. It can be supposed that LSA particles influence the curing process, not allowing to reach perfect cure. Under these conditions a certain grade of viscoelasticity could remain in the material, that can be responsible of nanoparticles flow at high loads, with consequent internal rearrangement and enhancement of conductivity due to the increased number of contacts among nanoparticles. In order to verify both theories, DSC, rheological measurements and specimens microstructure investigations were carried out, whose results are reported in the following subsections.

3.3 DSC Measurement

Calorimetric measurement were performed, in order to evaluate the curing behaviour of the two HSA_3 and LSA_4 self-monitoring systems. DSC measurements were carried out by dynamic heating, under the above described conditions, respectively on neat resin and resin

loaded with the two nanopowders (Table 7). Tg of cured systems was evaluated too (Table 8) .

Table 7

To complete the DSC analysis, isothermal heating measurements were carried out at 30°C, 60°C and 90°C. Table 8 reports the results, in which the final degree of cure α (defined as the ratio between isothermal heat and total dynamic heat of reaction) is calculated for every system. The measurements of heat of reaction for the filled systems (epoxy + HSA and epoxy + LSA), both in dynamic and isothermal tests, were done normalizing the experimental value to the specific nanoparticles content.

Table 8

The thermal analysis demonstrated that the curing behaviour of all systems is very similar, even if in the case of filled systems the heat produced is reduced of an amount at least equivalent to the percentage of filler content. Moreover, in agreement with literature [41,42,43], it was found that the presence of thermally conductive filler decreases peak temperature of few degrees [44]. The degree of cure is higher at 60°C than 30°C, as expected, while the decrease of conversion at 90°C can be explained considering the plausible evaporation of the hardener at the high temperatures. In any case, no outstanding differences were found in the final degree of cure of samples

containing the two nanoparticles, at least not enough to justify the different self-monitoring behaviour due to the presence of uncured areas in LSA specimens.

3.4 Rheological Measurement

Rheological measurements were carried out in order evaluate the efficiency of carbon nanoparticles dispersion of HSA_3 and LSA_4 samples [45,46]. In Figure 6 complex viscosity ($\eta^* = \eta' - i\eta''$) as a function of angular frequency (ω) is reported. As commonly known [47], η' and η'' are respectively given by the

$$\eta' = \frac{G''}{\omega} \quad \text{and} \quad \eta'' = \frac{G'}{\omega} \tag{3}$$

with G' elastic or storage modulus and G'' viscous or loss modulus.

Figure 6

G' and G'' for samples with different nanofillers are plotted in Figures 7.

Figure 7

The results show that the two specimens present pretty much the same viscosity, nevertheless, considering that HSA_3 sample contains a much lower filler content, it is possible to conclude that it presents a more uniform filler dispersion. The literature [48] suggested a method to quantify the dispersion level of nanoparticles in a polymeric matrix with the evaluation of the shear thinning effect in polymer– nanoparticles viscosity curves. Clear correlation between the shear thinning exponent *n* and the tensile modulus can be done: the higher the exponent *n*, the more efficient and well dispersed is the reinforcement of the respective composite. Higher values of viscosity and G'' for the HSA system confirm that, for the CnPs dispersions, higher surface area of HSA particles gives better dispersion of the nanoparticles in the epoxy system.

3.5 Microstructure

SEM micrographs of HSA_3 and LSA_4 bulk specimens (Figure 8), taken following the suggestions reported in [49], confirm that the two systems present different microstructures. In particular, a more uniform filler distribution is achieved in the case of HSA_3 specimens, where the dark areas, related to the presence of carbon nanoparticles, are well dispersed throughout the specimen. LSA microstructure, instead, is composed of more coarse and compacted nanoparticles agglomerates surrounded by neat resin (white areas) that, anyhow, form a continuous patter that allow electrical conductivity. These observations strengthen the theory that considers filler dispersion the major feature affecting self-monitoring properties, more that its interaction with the resin. In the case of LSA_4 samples, in fact, carbon nanoparticles form "low structure" aggregates, with few connections among each others. In our opinion such aggregates under high loads collapse releasing nanoparticles that start to contribute to electrical conductivity and hence, leading to the electrical resistance recovery.

Figure 8

4. Conclusions

In this paper, two self-monitoring hybrid composite materials, containing different carbon nanoparticles as conductive phase, were prepared and tested. The results showed that only HSA samples containing high surface area nanoparticles show true self-monitoring behaviour, while low surface area nanoparticles are not suitable for such applications, since electrical resistance recovery was found at high loads. DSC measurements evidenced that both types of nanoparticles do not interact with resin cure. Rheological measurements demonstrated that HSA samples show a more uniform filler dispersion, while large aggregates are present in the case of LSA ones. This occurrence

could be responsible for the electrical resistance recovery, due to aggregates breakage at high loads, with consequent release of a number of carbon nanoparticles in the matrix, that increase electrical conductivity. SEM observations confirm the different microstructures of the two types of specimens, validating this theory.

Finally, it is possible to conclude that the main result of the performed research is that conductive filler dispersion and its intrinsic properties are very important features when aimed to prepared self-monitoring materials. In particular, the use of nanofillers with high surface areas, high OAN and low particle dimensions are recommended to achieve a reliable self-monitoring system.

References

[1] Schulte K, Baron C. Load and failure analyses of CFRP laminates by means of electrical resistivity measurements, Comp. Sci and Tech. 1989; 36**:**63-76

[2] Chung DDL. Structural Health monitoring by electrical resistance measurement Smart Mater.Struct. 2001; 10:624-636

[3] Muto N, Arai Y, Shin SG, Matsubara H, Yanagida H, Sugita M et al. Hybrid composites with self-diagnosis function preventing fatal fracture. Comp Sci. and Tech. 2001; 61:875-883

[4] Micelli F, Nanni A Durability of FRP rods for concrete structures Construction and Building Materials 2004;18:491-503

[5] Wu ZS, Yang CQ, Harada T, Ye LP. Self-Diagnosis of structures strengthened with hybrid carob-fibre-reinforced polymer sheets Smart Mater. Struct. 2005; 14:S39-S51

[6] Tracy M, Chang FK. Identifying Impact Load in Composite Plates Based on Distributed Piezoelectric Sensors Proc. of SPIE Smart Structures and Materials Conference, San Diego (California USA),1996; 2779:118-23

[7] Zhou Z, Ou JB, Wang B. Smart FBG-OFBG bars and their applications in reinforced concrete beams in Structural Health Monitoring and Intelligent Infrastructures, Proc.of the First international Conference on Structural Health Monitoring and Intelligent Infrastructures, Tokyo (Japan) 2003; 861-866

[8] Kabashima S, Ozaki T, Takeda N. Damage detection of satellite structures by optical fiber with small diameter; Proc. SPIE San Jose (California, USA) 2000; 3985: 343–51

[9] Indada H, Okuhara Y, Kumagai H, Health monitoring of concrete structure using self-diagnosis materials. In: F. Asari, editor. Sensing Issues in Civil structural Health Monitoring, Berlin, Springer; 2005, 239-248

[10] Nanni F, Auricchio F, Sarchi F, Forte G, Gusmano G. Self-sensing CF-GFRP rods as mechanical reinforcement and sensors of concrete beams. Smart Mater. Struct. 2006; 15:182-186

[11] Li C, Thostenson ET, Chou TW Sensors and actuators based on carbon nanotubes and their composites: a review. Comp. Sc. and Tech. 2008; 68:1227-1349

[12] Okuhara Y, Matsubara H. Memorizing maximum strain in carbon-fiber-reinforced plastic composites by measuring electrical resistance under pre-tensile load. Comp. Sc. and Tech. 2006; 65:2148-2155

[13] Nanni F, Ruscito G, Madau F, Gusmano G. Self-sensing polymer composite materials for civil applications. keynote lecture Proc. PPS 24 The Polymer Processing Society 24th Annual Meeting - Salerno, Italy, 2008; S11: 793-796

[14]Wang S, Chung DDL. Interlaminar interface in carbon fibre polymer-matrix composites, studied by contact electrical resistivity measurement. Composite Interfaces, 1999; 6(6):497-506

[15] Todoroki A, Yoshida J. Electrical resistance change of unidirectional CFRP due to applied load JSME International Journal, Series A: Solid Mechanics and Material Engineering, 2004; 47(3): 357-364

[16] Ji Ho Kang, Paty S, Kim RY, Tandon GP. Self-diagnosis of damage in fibrous composites using electrical resistance measurements, proc. SPIE, 2006; Vol. 6176, 617602-1-12

[17] Okuhara Y, Matsubara H. Carbon-matrix composites with continous glass fiber and carbon black for mazimum strain sensing, Carbon, 2007;45: 1152-1159

[18] Nanni F, Ruscito G, Gusmano G. Assessment of self-diagnosis properties of CP_GFRP nanocomposites for civil applications, Proc. ICCST 6, Sixth International Conference on Composite Science and Technology Durban, South Africa,2007;

[19] Okuhara Y, Jang BK, Matsubara H, Sugita M. Fiber reinforced composites as self-sensing materials for memorizing damage histories, Proc. SPIE Smart Structures and Materials Proceedings, San Diego (California, USA), 2003; 314-322

[20] Thostenson ET, Chou TW Carbon nanotubi networks: sensing of distributed strain and damage for life prediction and self-healing, Advanced Materials, 2006;18:2837-2841

[21] Gao L, Thostenson ET, Zhang Z, Chou TW Coupled carbon nanotube network and acoustic emission monitoring for sensing of damage development in composites, Carbon, 2009;47:1381-1388

[22] Bakis CE, Nanni A, Terosky JA. Koehler S.W. Self monitoring, pseudo-ductile, hybrid FRP reinforcement rods for concrete applications, Comp. Sc. and Tecn.,2001; 61:815-823

[23] Krestis G. A review of the tensile, compressive, flexural and shear properties of hybrid fibre-reinforced plastics. Composites,1987; 18:13-23

[24]Nanni F, Ruscito G, Forte G, Gusmano G. Design, manufacturing and testing of sel-sensing carbon fibre-glass fibre reinforced polymer rods, Smart Mater. Struct. 2007; 16: 2368-2374

[25] Wang S, Kowalik DP, Chung DDL Self-sensing attained in carbon-fiber-polymer-matrix structural composites by using the interlaminar interface as sensor Smart Mater. Struct. 2004;13:570–592

[26] Okuhara Y, Shin SG, Matsubara H, Yanagida H, Takeda T. Self-diagnosis function of FRP containing electrically conductive phase, Proc. of SPIE's Sensory Phenomena and Measurements Instrumentation for Smart Structures and Materials, San Diego (California, USA),2000; 191-198

[27] Okuhara Y, Shin SG, Matsubara H, Yanagida H, Takeda T, Development of conductive FRP containing carbon phase for self-diagnosis structures Proc. of SPIE's Smart Structures and Materials, New Port Beach (California, USA) 2001; 314-322

[28] Thostenson ET, Chou TW Real-time in situ sensing of damage evolution in advanced fiber composites using carbon nanotube networks, Nanotechnology, 2008;19:215713-9

[29] Chou TW, Gao L, Thostenson ET, Zhang Z, Byun JK Real-time in situ sensing of damage evolution in advanced fiber composites using carbon nanotube networks , Comp. Sci and Tech. 2010;70:1-19

Dharap P, li Z, Nagarajaiah S, Barrera EV. Nanotube film based on single-wall carbon nanotubes for strain sensing, Nanotechnology 2004;15:379-382

[30] Park M, Kim H, Youngblood JP. Strain-dependent electrical resistance of multi-walled carbon nanotube/polymer composite films, Nanotechnology 2008;19:055705 (7pp)

[31] Wichmann M.H.G., Buschhorn S.T., Gehrmann J, Schulte K Piezoresistive response of epoxy composites with carbon nanoparticles under tensile load, Phys. Rev. B 2009; 80: 245437

[32] Kirkpatrik S. Percolation and Conduction, Reviews of Modern Physics 1973; 45(4):574-588

[33] Brosseau C, Boulic F, Queffelec P, Bourbigot C, Le Mest Y, Loaec F, et al. Dielectric and microstructure properties of polymer carbon black composites, J. Appl. Phys. 1997; 81 (2): 882-891

[34] Mallette JG, Quej LM, Marquez A, Manero O. Carbon black-filled PET/HDPE blends: effect of CB structure on rheological and properties, J. of App. Pol. Sci., 2001;81:562-569

[35] Traina M, Pegoretti A, Penati A. Time temperature dependence of the electrical resistivity of high density polyethylene/carbon black composites, J. of App. Pol. Sci., 2007;106; 2065-2074.

[36] Balberg I. A comprehensive picture of the electrical phenomena in carbon-black polymer composites, Carbon, 2002; 40:139-143

[37] Keithely appl. Note number 2418, 2004

[38] Flandin U, Prasse T, Schueler R, Schulte K, Bauhofer W, Cavaille JY Anomalous percolation transition in carbon black –epoxy composite materials, Phys. Review B, 1999,59(22):14349-14355

[39] Janzen J. On the critical conductive filler loading in antistatic composites, J.Appl.Phys. 1975; 46: 966-969

[40] Donnet JB, Bansal RC, Wang M.J. Carbon Black, Mercel Dekker Inc, 1993

[41] Valentini L, Armentano I, Puglia D, Kenny J. Dynamics of amine functionalized nanotubes/epoxy composites by dielectric relaxation spectroscopy, Carbon, 2004;42:323-329

[42] Tao K, Yang S, Grunlan JC, Kim YS, Dang B, Deng Y, et al. Effects of carbon nanotube fillers on the cuuring processes of epoxy resin-based composites, J. of App. Pol. Sci. 2006;102:5248-5254

[43] Chung DDL. Calorimetric study of the effect of carbon fillers on the curing epoxy, Carbon 2004;42:3003-3042

[44] Xie H, Liu B, Sung Q, Kim YS, Yuan Z, Shen J, et al. Cure Kinetic Study of Carbon Nanofibers/Epoxy Composites by Isothermal DSC, J. of App. Pol. Sc., 2005;96:329-335

[45] Khare R, de Pablo JJ, Yethiraj A, Rheology of Confined Polymer Melts, Macromolecules, 1996;29(24):7910-7918

[46] Lakdawala K, Salovey R. Rheology of Polymers Containing Carbon Black, 1987, Polymer Engineering and Science 1996:27 (14): 1035 - 1042

[47] Gandhi K, Salovey R. Dynamic and Mechanical Behaviour of Polymer Containing Carbon Black, Polymer Engineering and Science, 1988;28:877-887

[48] Wagener R, Reisinger TJG. A rheological method to compare the degree of exfoliation of nanocomposites, Polymer 2003;44 (24): 7513 - 7518

[49] Kovacs JZ, Andresen K, Pauls JR, Garcia CP, Schossig M, Schulte K, et.al. Analyzing the quality of carbon nanotube dispersions in polymers using scanning electron microscopy. Carbon 2007;45(6):1279-1288

LIST OF CAPTIONS

Figure 1 Error! Main Document Only. (a) Sketch of hybrid CnP-GFRP, (b) sample cut and open to show inner part and (c) SEM micrograph of the internal conductive core cross section (CnP in epoxy resin + glass fibres)

Figure 2 LSA (dotted curve) and HSA (continuous curve) in epoxy percolation curves

Figure 3 Self-monitoring results for HSA_3 sample. Load/time curve (light gray line) and $\Delta R/R_0$% /time curve (dark gray line) both under continuous and cyclic loading

Figure 4 Self-monitoring results for LSA_4 specimens: Load/time curve (light gray line) and $\Delta R/R_0$% /time curve (dark gray line) both under continuous and cyclic loading.

Figure 5 Stress/strain curve (dotted light gray line) and $\Delta R/R_0$% /strain curve (dark gray line) for a) HSA_3 sample, b) LSA_4 sample. Electrical resistance variation against strain up to 1%strain are reported in figure c) for both specimens.

Figure 6 Viscosity of HSA_3 and LSA_4 samples as a function of angular frequency.

Figure 7 G' and G'' of HSA_3 and LSA_4 samples as a function of angular frequency

Figure 8 FEG-SEM micrographs of HSA_3 and LSA_4 cured specimens

TABLES

Table 1 Specimens main characteristics

Internal conductive core diameter (mm)	*Total diameter (mm)*	*Specimens length (mm)*	*Fibre volume fraction in conductive core*	*Fibre volume fraction in external sheaths*
1.3±0.2	3±0.4	200±8	0.53±0.04	0.62±0.05

Table 2 Carbon nanoparticles main characteristics

Carbon nanoparticles	*Supplier*	*Surface area (BET) [m^2/g]*	*OAN* (ASTMD2414-04) *[cm^3/g]*	*Density (ρ)*	*Particle size [nm]*
Printex XE 2B	Degussa	1000	3.8	130 *[g/dm^3]*(Pour ASTM D1513)	30
Super P	Timcal	62	2.9	160 *[kg/m^3]*(in the bag, Int. method26)	40

Table 3 Carbon nanoparticles content in manufactured samples

CnP type	*Acronym*	*Sample #*	*CnP (% Vol)*
Xe-2B	HSA_# (High Surface Area)	HSA_1	1.2±0.15
		HSA_2	1.7±0.17
		HSA_3	2.2±0.12
		HSA_4	2.7±0.16
		HSA_5	3.7±0.22
		HSA_6	4.7±0.18
Super P	LSA_# (Low Surface Area)	LSA_1	2±0.13
		LSA_2	3±0.18
		LSA_3	3.5±0.2
		LSA_4	3.8±0.23
		LSA_5	4.5±0.28
		LSA_6	6±0.38

Table 4 Electrical resistivity measurements for HSA and LSA samples (measurements repeated on three samples of each type)

HSA		*LSA*	
Sample #	***Resistivity ρ [Ω*cm]***	***Sample #***	***Resistivity ρ [Ω*cm]***
HSA_1	Insulator	LSA_1	Insulator
HSA_2	Insulator	LSA_2	Insulator
HSA_3	495±50	LSA_3	9850±1580
HSA_4	304±15	LSA_4	470±59
HSA_5	275±17	LSA_5	115±7.8
HSA_6	89±3.5	LSA_6	70±6

Table 5 Percolation Threshold obtained by Janzen Equation and experimental data for both systems

Sample	***Φ_C (Vol %) Janzen Value***	***Φ_C (Vol %) Experimental Value***
HSA_3	3.3	2.2
LSA_4	4.3	3.8

Table 6 Main mechanical and self-monitoring results of HSA_3 and LSA_4 type samples (tests repeated on 3 different specimens of each type)

Sample	**Initial Electrical Resistance (kΩ)**	**Maximum Load (N)**	**Specimen cross section (mm^2)**	**Tensile strength (MPa)**	**Maximum Strain (%)**	**Electrical Resistance Variation at fracture(%)**	**Strain @ 1000N (%)**	**Electrical Resistance Variation @1000N(%)**
HSA_3	290±16	7365±203	21±0.7	347±21	3±0.36	32 ±4.5	0.24±0.05	0.8±0.3
LSA_4	330±20	6882±110	22±0.8	313±16	4.1±0.55	13* ±5.5	0.33±0.06	0.9±0.4

*Maximum electrical resistance variation during test =16.44%±1.6 @≈5000N

Table 7 Results of dynamic heating of HSA and LSA systems.

	ΔH (J/g)	**T_{peak} (°C)**	**T_g (°C)**
Epoxy	512.90±11. 3	96.7±1.1	96.7±1.0
Epoxy + HSA_3	415.04±9.8	95.2±0.8	96.4±0.9
Epoxy + LSA_4	401.01±0.3	94.2±1.2	95.8±1.1

Table 8 Results of isothermal heating of HSA and LSA systems.

	T_{iso} = 30°C	**T_{iso} = 60°C**	**T_{iso} = 90°C**

	ΔH (J/g)	**t_{peak} (min)**	**α**	**ΔH (J/g)**	**t_{peak} (min)**	**α**	**ΔH (J/g)**	**t_{peak} (min)**	**α**
Epoxy	446.43	9.72	0.87	435.93	2.07	0.87	448.01	0.49	0.87
Epoxy + HSA_3	412.86	5.37	0.80	434.33	1.04	0.84	387.01	0.74	0.75
Epoxy + LSA_4	389.89	8.15	0.76	421.19	1.40	0.82	387.47	0.74	0.76

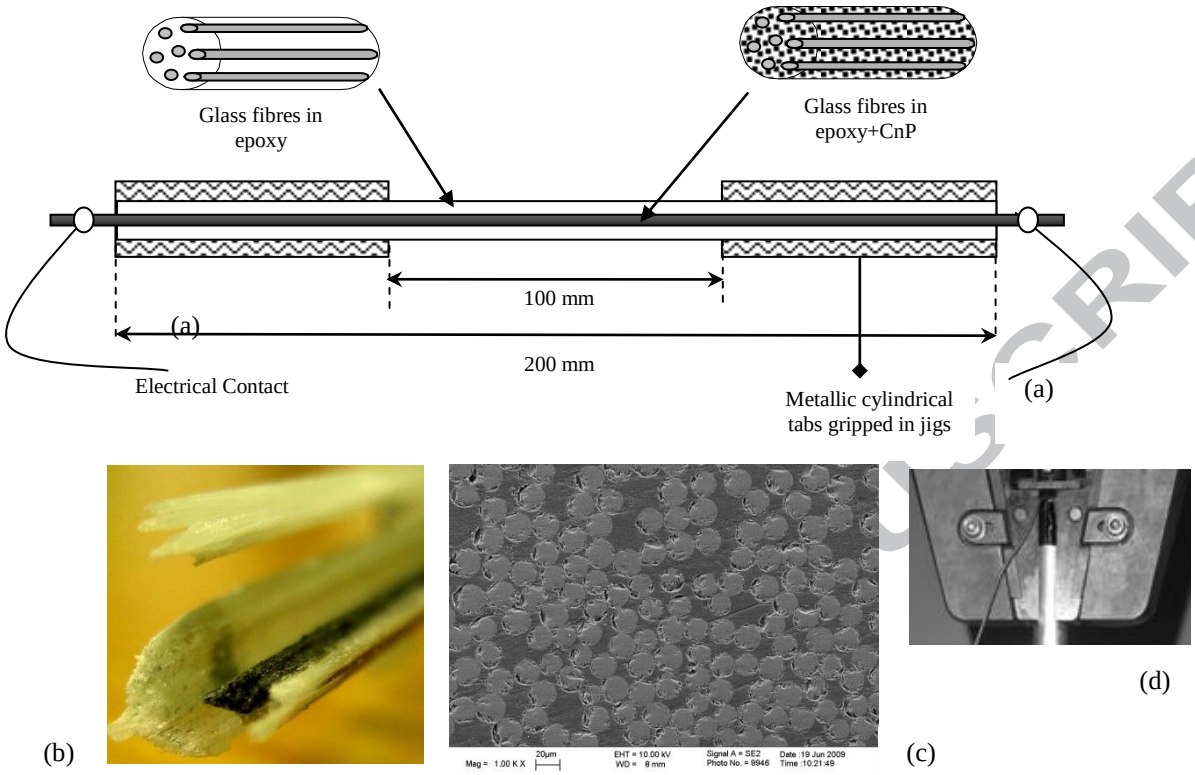

Figure 1 (a) Sketch of hybrid CnP-GFRP, (b) sample cut and open to show inner part, (c) SEM micrograph of the internal conductive core cross section (CnP in epoxy resin + glass fibres) and (d) particular of sample gripping in tensile test jags

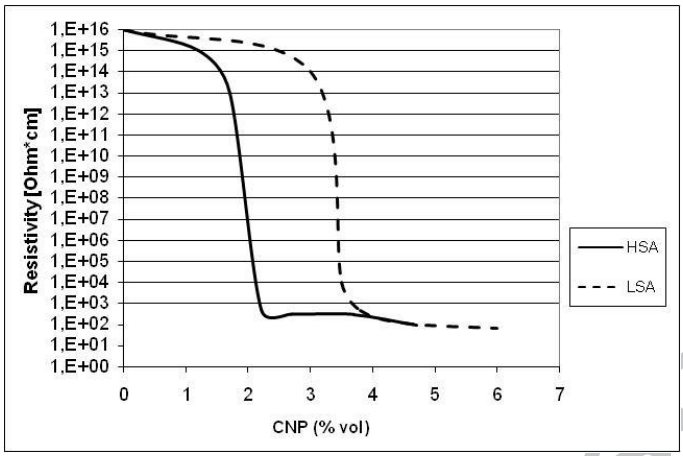

Figure 2 LSA (dotted curve) and HSA (continuous curve) in epoxy percolation curves

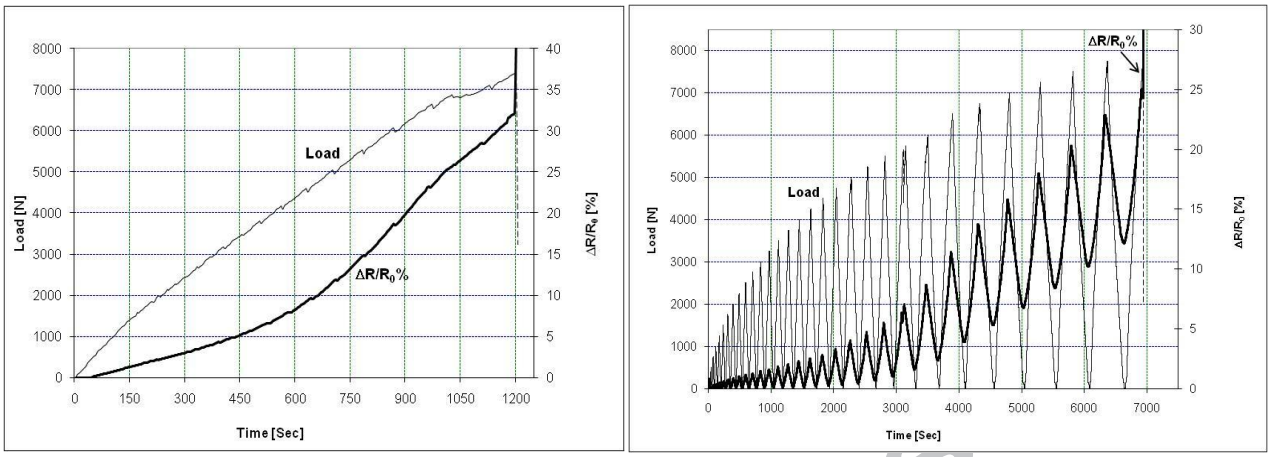

Figure 3 Self-monitoring results for HSA_3 sample. Load/time curve (light gray line) and $\Delta R/R_0$% /time curve (dark gray line) both under continuous and cyclic loading

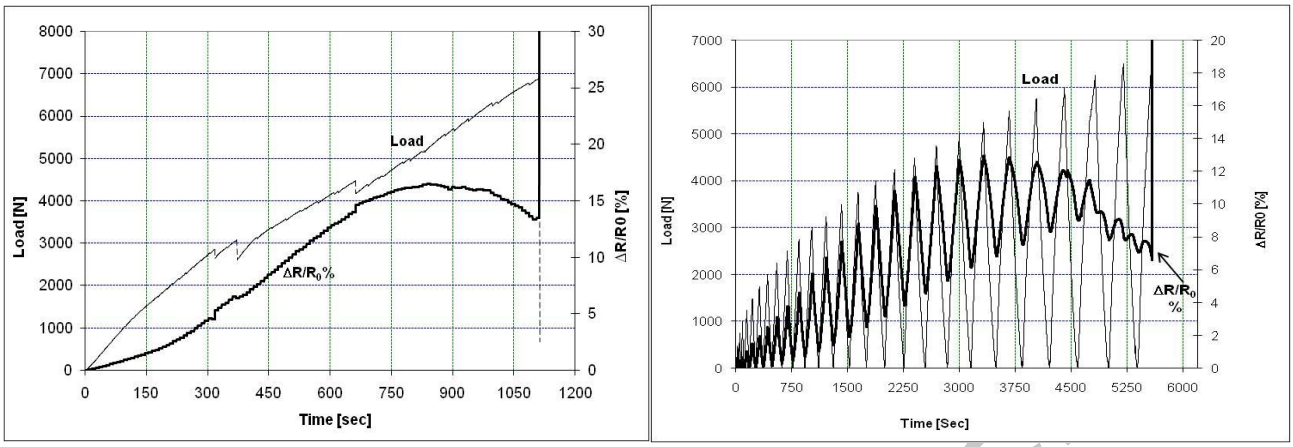

Figure 4 Self-monitoring results for LSA_4 specimens: Load/time curve (light gray line) and $\Delta R/R_0$ % /time curve (dark gray line) both under continuous and cyclic loading.

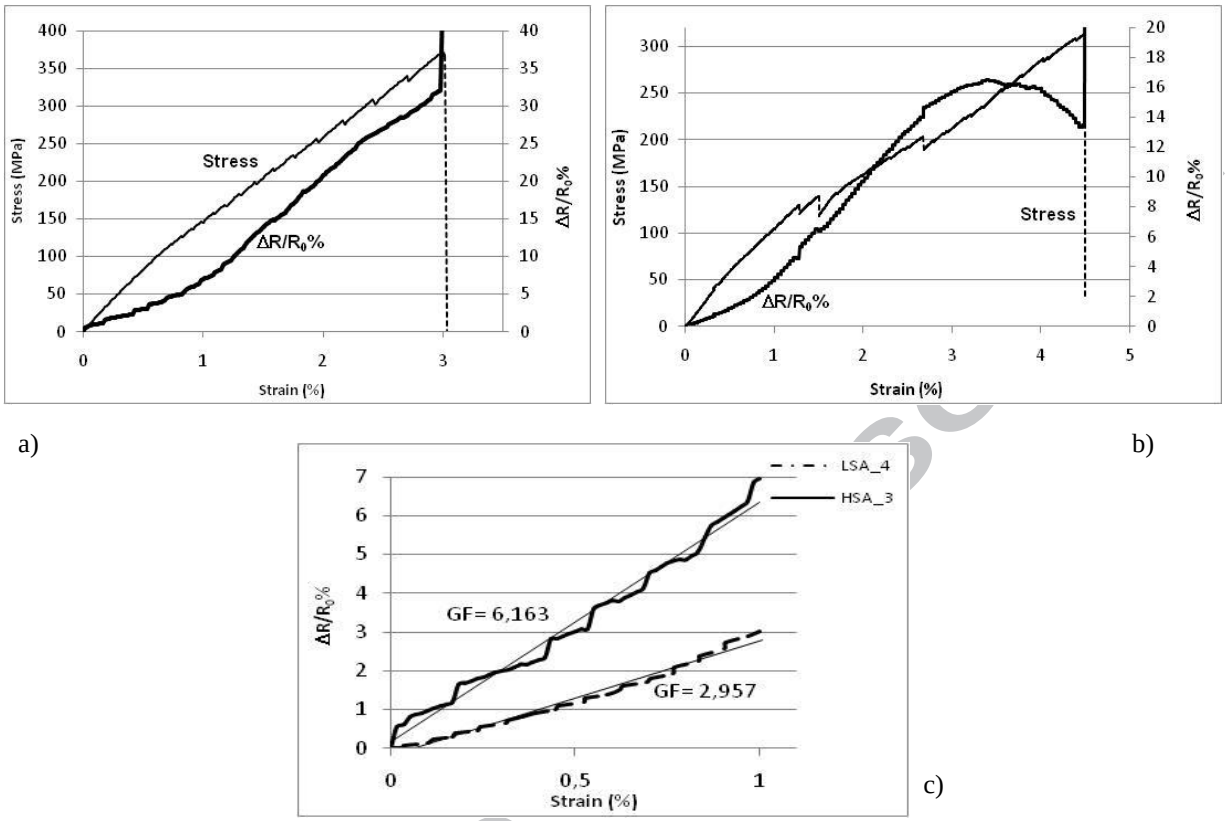

Figure 5 Stress/strain curve (dotted light gray line) and $\Delta R/R_0$% /strain curve (dark gray line) for a) HSA_3 sample, b) LSA_4 sample. Electrical resistance variation against strain up to 1%strain are reported in figure c) for both specimens.

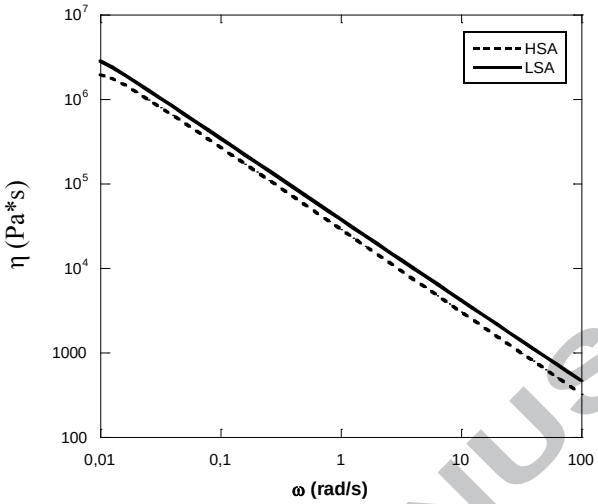

Figure 6 Viscosity of HSA_3 (dotted line) and LSA_4 (continuous line) samples as a function of angular frequency.

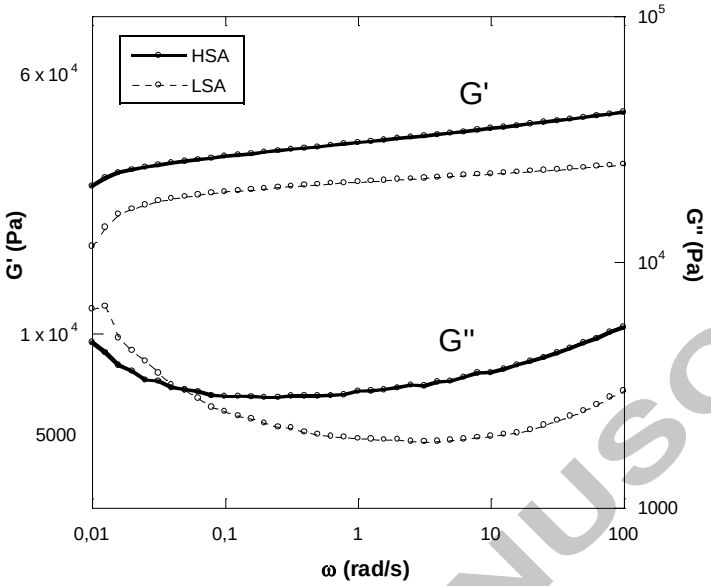

Figure 7 G' and G'' of HSA_3 (continuous dark curve) and LSA_4 (empty circles) samples as a function of angular frequency

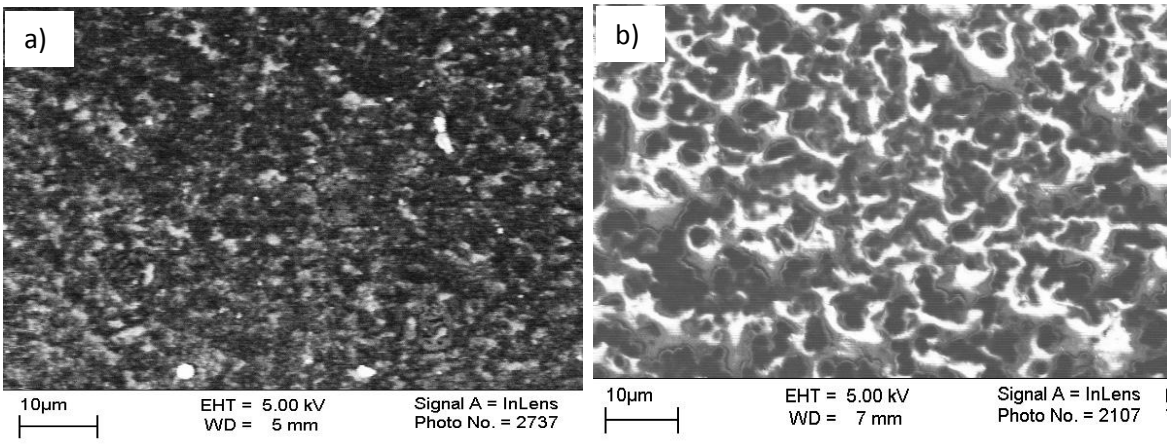

Figure 8 FEG-SEM micrographs of (a) HSA_3 and (b) LSA_4 cured specimens